Bull. Inst. Chem. Res., Kyoto Univ., Vol. 66, No. 5, 1988

Structure of Metal-Phthalocyanine Polymer Studied by High Resolution Electron Microscopy and Electron Energy Loss Spectroscopy

Takashi KOBAYASHI*, Hiroki KURATA*,
Takashi MAEDA* and Noboru KAWASE*

Received December 1, 1988

Structure of SiO-phthalocyanine (SiOPc) polymer obtained by dehydration of $Si(OH)_2$-derivative has been studied by direct imaging of molecular images and electron energy loss spectroscopy. It has been found that the crystal has a mosaic structure and polymer chains are along two directions in the crystal. In the chain, each SiPc molecule stack cofacially but in staggering state and the molecular planes are perpendicular to the polymer chain. Electron energy loss spectra was also measured and its anisotropic behavior was interpreted on the basis of the crystal structure.

KEY WORDS: Conductive polymer/ Crystal structure/ Phthalocyanine-siloxane polymer/ EELS/ Molecular images/

INTRODUCTION

Metal derivatives of phthalocyanine are spotlighted because of their high electric conductivity in partially oxidized states[1,2]. Especially the Si- or Ge-derivatives crystallize as stable oxy-linked polymers and their iodine-doped samples show metallic conductivity[3,4]. Dirk et al.[5] have studied these materials extensively by spectroscopic method and X-ray powder diffractometry and proposed some models for the structures of the Si- and Ge-polymer derivatives. In 1988, we have reinvestigated these materials in the form of thin epitaxial films by direct imaging of the molecules by high resolution electron microscopy[6,7]. The results differ in some parts from those reported by Dirk et al.. However, they studied the fine powdery crystals while we used the epitaxial films prepared by vacuum deposition on clean surface of KCl single crystals. The epitaxial method happens to produce sometimes a new crystal form, polymorph, due to the interaction between the atoms of the substrate and the molecules deposite on it. Therefore, we have tried to study the structure of the fine crystalline particles of the powder prepared by the same method used by them.

Two different modes of the stacking have been proposed[3,8] for the oxy-linked polymers of phthalocyanine derivatives. One is that where the phthalocyanine ligands stack cofacially forming a polymer chain but staggered each other relative to the upper or the lower ones in the chain. The other is that where the staggering angle is zero and the ligand eclipses the neighboring one. The both states are

* 小林隆史, 倉田博基, 前田尚志, 川瀬 昇 : Laboratory of Crystal and Powder Chemistry, Institute for Chemical Research, Kyoto University, Uji, Kyoto 611.

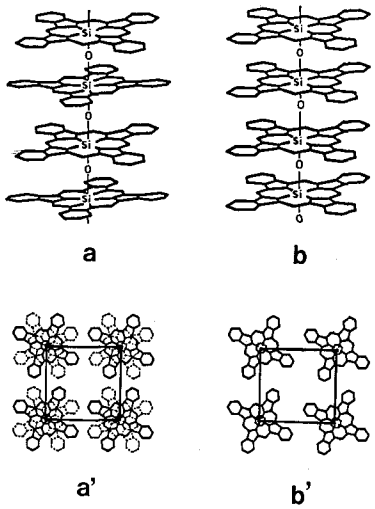

Fig. 1. Two different structures proposed for the oxylinked phthalocyanine polymers. (a) shows alternate stacking in staggering state (Ref. 5) and (b) shows eclipsed state (Ref. 8). (a) (b) are the projections of the polymer chains. (a′) and (b′) along the chain axis.

shown in Fig. 1.

EXPERIMENTAL

Powder of $(SiOPc)_n$ prepared by dehydration of $SiPc(OH)_2$ crystals in vacuum was dispersed in water and a drop of the suspension was dried on a microgrid for the observation with an electron microscope equipped with a magnetic sector-type electron energy analyzer. Theoretical resolution of the EM is 2.0 Å and the energy resolution of the analyzer is 2 eV. The energy analyzer used was the JEOL-ASEA2 with a serial detection system mounted under JEOL-100C EM[9]. For the observation of the images of the polymer chain JEOL-200C top entry-type EM having a minimum dose system was used which can protect the specimens from the electron irradiation damage before recording the images.

RESULTS AND DISCUSSION

a) Electron microscopy

Fig. 2 is an electron micrograph showing an elongated flake of $(SiOPc)_n$ crystal mounted on a hole of the gold-coated microgrid. The inset is the enlarged micrograph of the part encircled which shows the lattice fringes whose intervals are 13.7 Å. The fringes run along the long axis of the crystal and this feature resembles to the images of ClAlPc reported by Kenney et al.[10]. The selected area electron diffraction pattern from this crystal is reproduced in Fig. 3. The diffraction pattern exhibits a fiber structure and very intense diffraction spots are observed with a period of 3.3 $Å^{-1}$. Phthalocyanine ligand has in general the sizes of about 13 Å × 13 Å × 3.4 Å according to the data on many metal derivatives

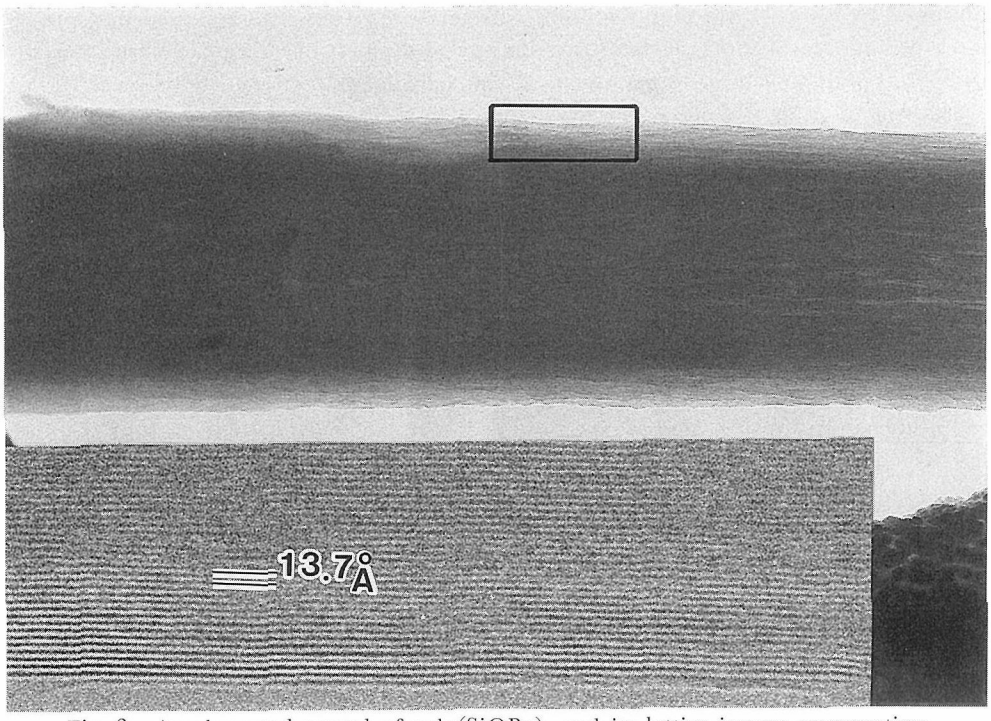

Fig. 2. An elongated crystal of poly(SiOPc)$_n$ and its lattice images representing the polymer chains. The enclosed part is enlarged in the inset.

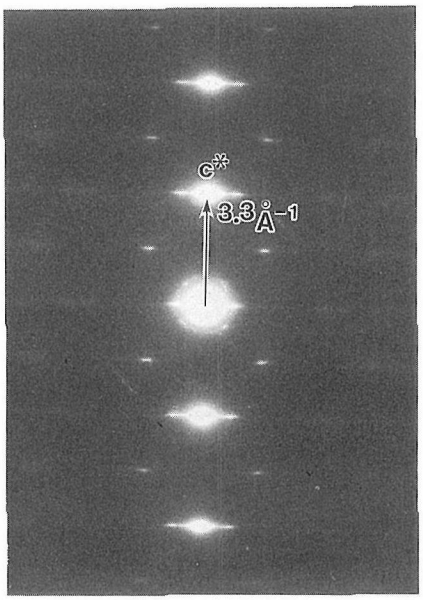

Fig. 3. Selected area electron diffraction pattern from the crystal shown in Fig. 2. The direction of the c*-axis is along the long axis of the crystal.

obtained by X-ray diffraction method[11]. Therefore, it may be assumed and proved later by high resolution electron microscopy and electron energy loss spectroscopy that the phthalocyanine ligands stack in parallel along the long axis of the crystallites with the spacing of 3.3 Å. The ligand planes can be considered to be almost perpendicular to this axis, so that they can produce the strongest diffraction to the direction of the stacking axis.

Fig. 4 (a, b) shows another but popular crystallite of the present specimen and its electron diffraction pattern. This fiber pattern also shows the same very strong diffraction spots on the meridian on alternate layer lines as can be seen in Fig. 2. The strongest spot on the second layer line corresponds to the interplanar lattice spacings of 3.3 Å. The direction along the meridian is tentatively taken as the c*-axis of the crystal according to Dirk et al. who have reported that the unit cell dimensions of the crystal are a=13.80 Å, b=27.59 Å, c=6.66 Å and Z=4 on the basis of X-ray powder diffraction pattern. They also proposed a plausible space group, Ibam, for the crystal to belong to. On the equator the diffraction spots are arrayed at the interval of $1/13.7\ \text{Å}^{-1}$ and therefore the direction along the equator may be assumed the a-axis of the crystal. Accordingly the pattern shown in Fig. 3 and 4 can be considered to be the projection along the b*-axis.

The diffraction spots on the equator, the first, the second and the third layers etc. are respectively indexed as (h00), (h01), (h02) and (h03) etc. where h's are all integers. The appearance of the layer lines of (h01) and (h03), that is the diffraction spots having the odd index for l at the (h01) diffractions are forbidden

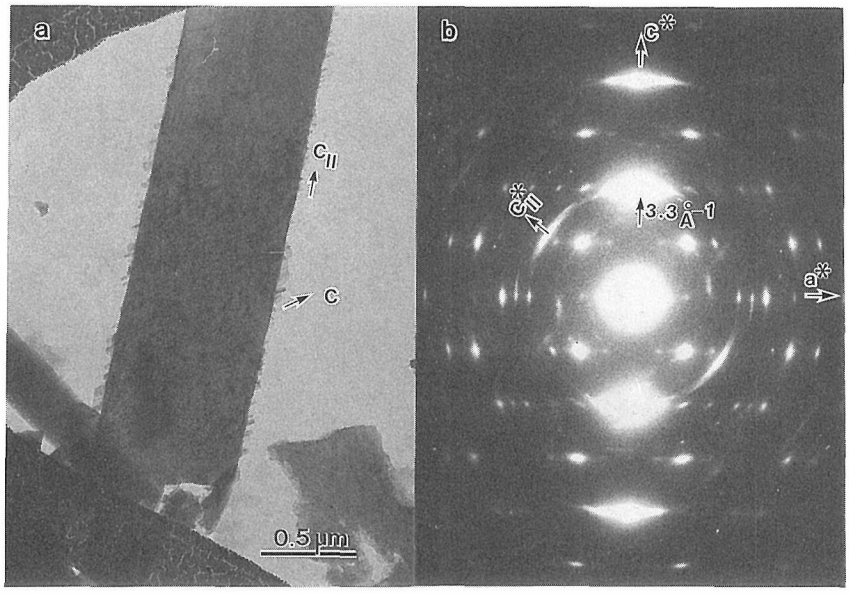

Fig. 4. Electron micrograph of poly(SiOPc)$_n$ crystal showing a mosaic structure (a) and the selected area electron diffraction from the crystal. The c*- and $c^*_{\parallel}$-axes in (b) coincide with the c- and $c_{\parallel}$-axes shown in (a).

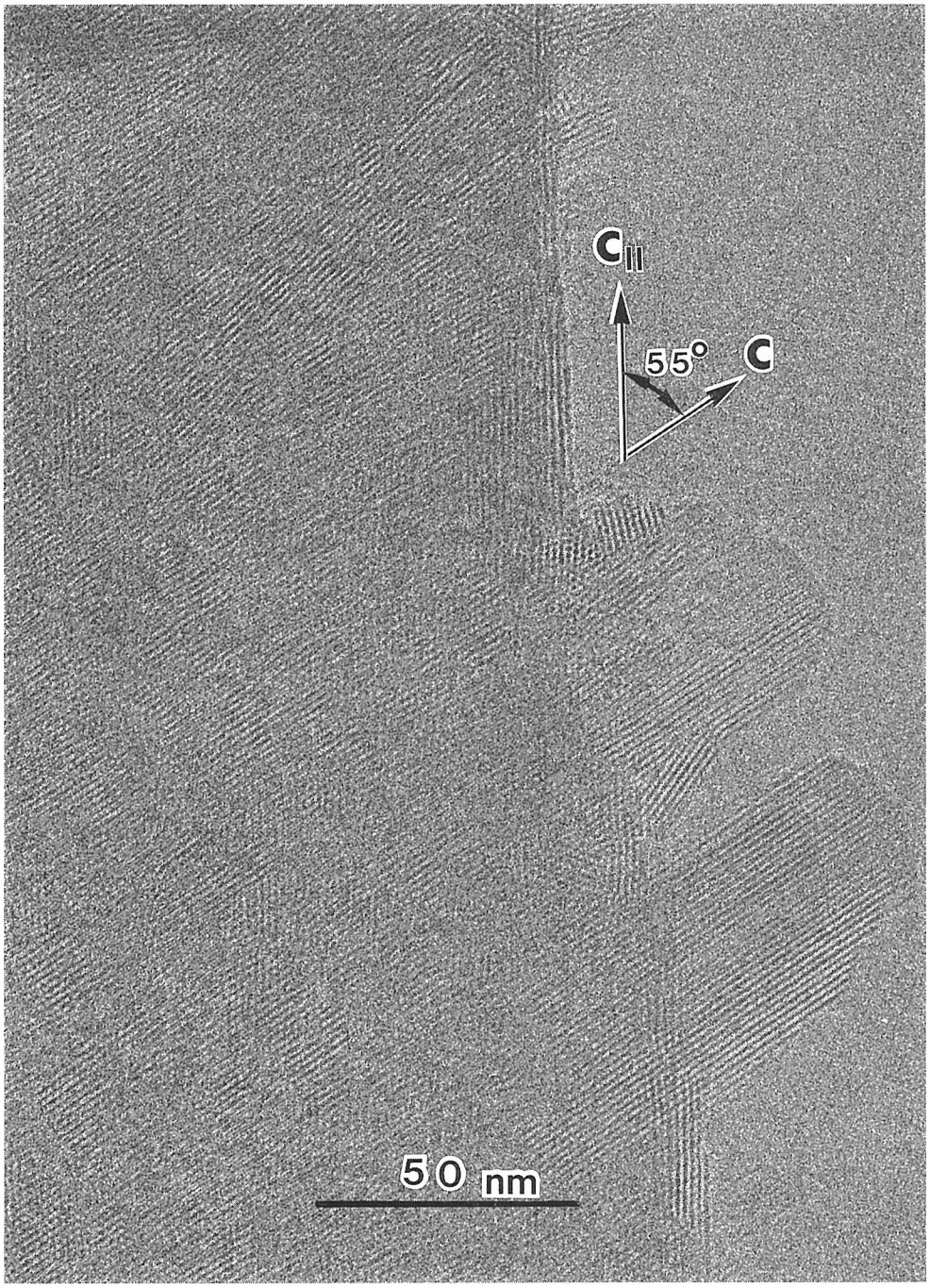

Fig. 5. High resolution electron micrograph of an edge part of the crystal shown in Fig. 4. The spacings of the lattice fringes are 13.7 Å in both the directions of c and $c_{\parallel}$.

for the crystal which belongs to the space group of Ibam. Therefore, another space group for this crystal seems to be suitable. Determination of the lattice symmetry from the electron diffraction are difficult and remains in future investigation.

The other characteristic of the diffraction patterns shown in Fig. 4 is the existence of two strong diffraction arcs. That is, two diffraction spots appear as arcs. The direction is designated here as $c^*_{\parallel}$-axis and coincides with the long axis of the crystal. The main c*-axis directs, therefore, 55° away from the long axis of the crystal. Many crystallites can be observed peeping from the edge of the fiber crystal, in the micrograph shown in Fig. 4(a). They orient in parallel and the direction of their fiber axis are same as that of the c*-axis. A part of the crystal edge was enlarged and reproduced in Fig. 5. The lattice frings with the spacing of 13.7 Å can be observed along the direction of the c*- and $c^*_{\parallel}$-axes. At the part of the mother crystal, fringes running along both directions are observed. The intensity distribution in the electron diffraction pattern (Fig. 4(b)) indicates that most of the fiber axes of the crystallites take the orientation directing the c*-axis and some small parts are in the direction along the $c^*_{\parallel}$-axis. Therefore, the crystals of poly-SiOPc obtained by dehydration of $Si(OH)_2Pc$ crystals are all

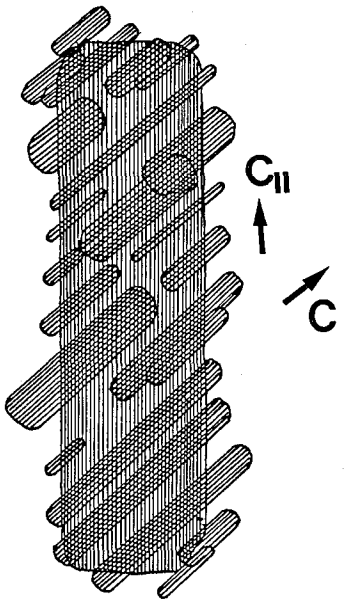

Fig. 6. Structure model of the mosaic crystal of poly$(SiOPc)_n$ obtained by dehydration of $Si(OH)_2Pc$. Such mosaic structure is produced during the polymerization and the original $Si(OH)_2Pc$ crystal does not exhibits such morphorogy.

mosaic as is schematically illustrated in Fig. 6. The reaction of the dehydration-polymerization seems to occur topotactic and the resultant products are composed of highly oriented smaller crystallites.

A part of the peeping crystallites are further enlarged and shown in Fig. 7. In every fringes having the spacings of 13.7 Å, finer lateral stripes also can be observed in the micrograph. The intervals between the successive stripes along the vertical direction are 3.3 Å which correspond to the spacings given by the strongest diffraction spots mentioned above. Each strip having the sizes of 13.7 × 3.3 Å^2 may be considered to be molecular image of SiPc projected along the molecular plane. They stack parallel forming a polymer chain. Oxygen combining two successive SiPc molecules should be found between two strips but it can not be detected in the micrograph. It is because of the low resolution of the present electron microscope (2.0 Å) and insufficiency for resolving it. The phase contrast of the oxygen is too low to detect.

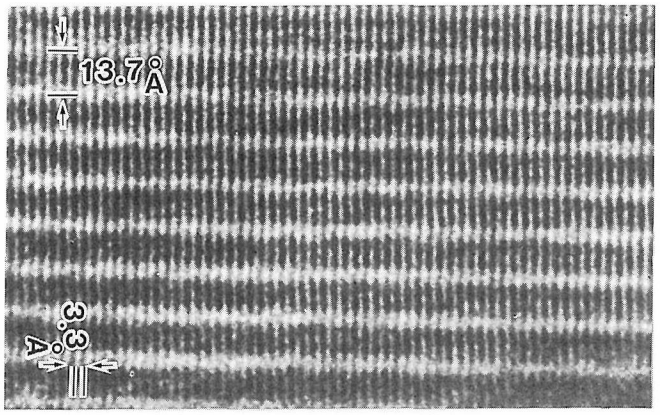

Fig. 7. High resolution electron micrograph showing the cofacial stacking of SiPc in the polymer chains.

It should be pointed out that in order to cause the diffraction spots having odd integers as the l-indices, alternately stacking SiPc should show two different projected images in the projection shown in Fig. 7. A laser optical diffraction pattern obtained from this image (Fig. 7) also exhibits the existence of such difffraction spots. This fact means that the molecular images shown in Fig. 7 contain the information concerning the difference in the projection of molecules but one can not visually recognize such difference in Fig. 7. The difference may be small and it may arise from a small deviation of a symmetrical axis or mirror plane running through the chain axis of the polymer from the direction of the principal crystal axis, b-axis. In Fig. 1 such symmetry elements are coincide with the crystal axes but if the model were true, the (h01) diffraction pattern should obey the extinction rule of $l=2n$ for all (h01) reflections.

In conclusion, the polymer chain of SiOPc are stacking along the c-axis of the crystal and the molecular planes of the phthalocyanine ligands (SiPc) are parpendicular to the axis. The distance between two successive ligands which are bound together by an oxygen is 3.3 Å. The stacking mode is the cofacial but staggering ones as shown in Fig. 1(a). This structure has been confirmed by electron energy loss spectra as is described in the following section.

b) *Electron energy loss spectra*

An electron energy analyzer connected with a transmission electron microccope has some advantages. One advantage is that an energy loss spectrum can be obtained from very small selected specimen area and another advantage is that the energy loss spectra can be obtained as a function of momentum transfer $\vec{q}$ for different directions of inelestically scattered electrons[13,14]. In the transmission electron microscope an amount of the momentum transfer $\vec{q}$ transferred at the time of the inelestic scattering can be detected at the back focal plane of the objective lens of the microscope where in usual case electron diffraction pattern is formed as a function of the scattering angles and directions. By inserting a small aperture at the diffraction plane one can select a specific region of $\vec{q}$. In one dimensional materials or other anisotropic substances, the electron energy loss spectra differ depending on the direction of $\vec{q}$[15,16]. It is not our present purpose to described such relationships in detail but the dependence of the spectra on the direction of the momentum transfer can be used to determine the molecular orientation in the specimen when the molecule itself is very anisotropic like the present specimen.

Fig. 8(b) shows the energy loss spectra of the poly-SiOPc crystal. The spectrum B was obtained from the encircled area by setting the objective aperture at B shown in Fig. 8(a), ie. $\vec{q}$ // c*-axis, while the spectra A was from the area A, ie. $\vec{q} \perp$ c*-axis as indicated in the figure. Two spectra show clear difference at low

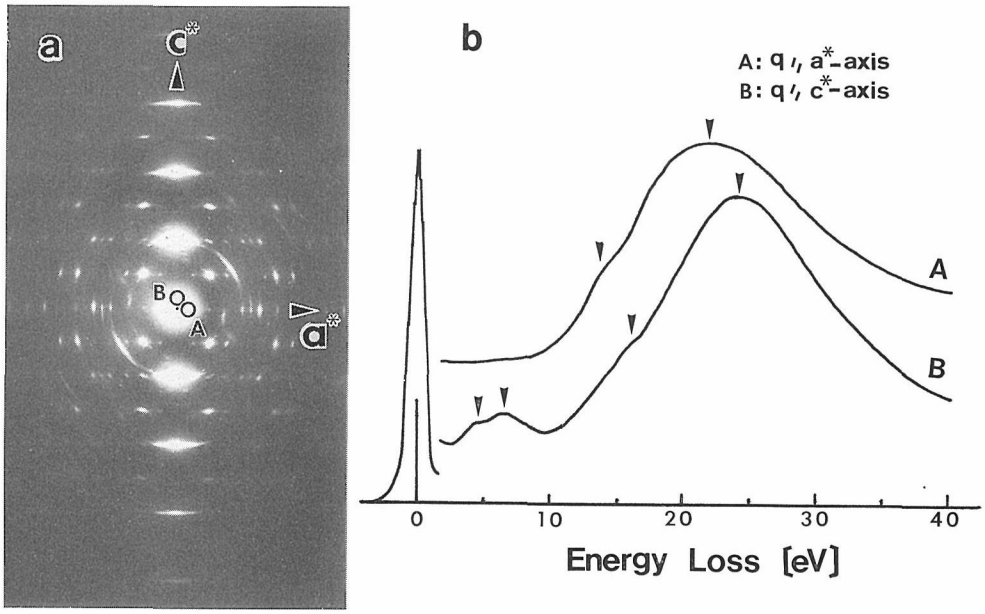

Fig. 8. (a) Electron diffraction pattern of poly(SiOPc)$_n$ and (b) electron energy loss spectra obtained by setting the objective aperture at A and B respectively in the diffraction plane as shown in (a). The aperture size is 5 μm in diameter which corresponds to the acceptance semi-angle of 1.36 mrad. and q=0.22.

energy loss region. Large and broad loss peaks near 20 eV are due to the excitation of plasmon loss of valence electrons as can be assigned from the analogy to the plasmon loss observed in graphite. Isaacson[17] has assigned the peaks to the overlapping of many intramolecular transitions of the electrons. The loss peaks appearing near 7 eV in the spectrum B bear resemblance to the loss peaks of graphite caused by the π-plasmon excitation reported by several authors. Zeppenfeld[18] has reported that the loss peak of graphite appeared at about 7 eV is due to the π-plasmon excitation and the energy values as well as its intensity vary depending on the momentum transfer $\vec{q}$. The intensity increases with decrease in angle between $\vec{q}$ and the c-axis of the graphite. That is, the loss peak appears with the highest intensity when the direction of the momentum transfer $\vec{q}$ is parallel to the c-axis and disappears when $\vec{q}$ is perpendicular to the axis. In the present case the peaks near 7 eV appears when $\vec{q}$ is parallel to the c*-axis of the poly-SiOPc crystal, that is, the selecting aperture is shifted along the c*-axis from the center, and disappear when $\vec{q}$ is perpendicular to the c*-axis, A. Phthalocyanine is a planar aromatic molecule and resembles a piece of cracked graphite layer. Therefore, it may be concluded that the molecular planes of SiPc are almost perpendicular to the c*-axis. The result agrees well with that obtained by high resolution electron microscopy and electron diffraction patterns as described above.

The detailed results about the dependence of the electron energy loss spectra of poly-phthalocyanines on the momentum transfer will be reported elsewhere.

ACKNOWLEDGEMENT

The authors wish to express their gratitude to Professor Emeritus Natsu Uyeda for his interest and encouragements throughout this work.

This work was supported in part by a grant in aid from the Ministry of Education of Japan for which we are deeply grateful.

REFERENCES

(1) J.L. Peterson, C.S. Schramm, D.R. Stojakovic, B.M. Hoffmann and T.J. Marks, *J. Am. Chem. Soc.*, **99**, 286 (1977).
(2) E. Canadell and S. Alvarez, *Inorg. Chem.*, **23**, 573 (1984).
(3) K. Schoch, Jr., B. Kundalkar and T. Marks, *J. Am. Chem. Soc.*, **101**, 7071 (1979).
(4) J. Martinsen, S. Palmer, J. Tanaka, R. Greene and B. Hoffman, *Phys. Rev.*, **B30**, 6269 (1984).
(5) C. Dirk, T. Inabe, K. Schoch and T. Marks, *J. Am. Chm. Soc.*, **105**, 1539 (1983).
(6) T. Kobayashi and N. Uyeda, *J. Cryst. Growth*, **84**, 589 (1987).
(7) T. Kobayashi and N. Uyeda, *Phil. Mag.*, **B57**, 493 (1988).
(8) E. Orthmann, V. Enkelmann and G. Wegner, *Makromol. Chem., Rapid Commun.*, **4**, 687 (1987).
(9) K. Ishizuka, H. Kurata, T. Kobayashi and N. Uyeda, *J. Electr. Micros.*, **35**, 343 (1986).
(10) J. Linsky, T. Paul, R. Nohr and M. Kenney, *Inorg. Chem.*, **19**, 3131 (1980).
(11) K. Wynne, *Inorg. Chem.*, **23**, 4458 (1984).
(12) K. Wynne, *Inorg. Chem.*, **24**, 1339 (1985).
(13) J. Silcox, *Ultramicros.*, **3**, 409 (1979).
(14) J. Silcox, 9-th Intern. Cong. Electr. Microsc., Toronto, **3**, 259 (1978).
(15) C. Chen, J. Silcox, A. Gartio, A. Heeger and A. MacDiarmid, *Phys. Rev. Lett.*, **36**, 525 (1976).

(16) J. Ritsuko, D. Sandman, A. Epstein, P. Gibbons, S. Schnatterly and J. Fields, *Phys. Rev. Lett.*, **34**, 1330 (1975).
(17) M. Isaacson, *J. Chem. Phys.*, **56**, 1803 (1972); 1813 (1972).
(18) K. Zeppenfeld, *Z. Phys.* **211**, 391 (1968).